Cubic spin-orbit coupling and anomalous Josephson effect in planar junctions

Mohammad Alidoust, Chenghao Shen, and Igor Žutić

Phys. Rev. B **103**, L060503 — Published 15 February 2021

DOI: 10.1103/PhysRevB.103.L060503

Cubic spin-orbit coupling and anomalous Josephson effect in planar junctions

Mohammad Alidoust,[1] Chenghao Shen,[2] and Igor Žutić[2]

[1] *Department of Physics, Norwegian University of Science and Technology, N-7491 Trondheim, Norway*
[2] *University at Buffalo, State University of New York, Buffalo, NY 14260-1500, USA*

(Dated: January 27, 2021)

Spin-orbit coupling in two-dimensional systems is usually characterized by Rashba and Dresselhaus spin-orbit coupling (SOC) linear in the wave vector. However, there is a growing class of materials which instead support dominant SOC cubic in the wave vector (cSOC), while their superconducting properties remain unexplored. By focusing on Josephson junctions in Zeeman field with superconductors separated by a normal cSOC region, we reveal a strongly anharmonic current-phase relation and complex spin structure. An experimental cSOC tunability enables both tunable anomalous phase shift and supercurrent, which flows even at the zero-phase difference in the junction. A fingerprint of cSOC in Josephson junctions is the f-wave spin-triplet superconducting correlations, important for superconducting spintronics and supporting Majorana bound states.

Spin-orbit coupling (SOC) and its symmetry breaking provide versatile opportunities for materials design and brining relativistic phenomena to the fore of the condensed matter physics [1–6]. While for decades SOC was primarily studied to elucidate and manipulate normal-state properties, including applications in spintronics and quantum computing [7–15], there is a growing interest to examine its role on superconductivity [16–21].

Through the coexistence of SOC and Zeeman field, a conventional spin-singlet superconductivity can acquire spin-dependent long-range proximity effects [20, 23, 24, 96] as well as support topological superconductivity and host Majorana bound states, a building block for fault-tolerant quantum computing [25–27]. In both cases, Josephson junctions (JJs) provide a desirable platform to acquire spin-triplet superconductivity through proximity effects [28–38]. In contrast, even seemingly well-established intrinsic spin-triplet superconductivity in Sr_2RuO_4 [39] is now increasingly debated [40, 41].

Extensive normal-state studies of SOC in zinc-blende heterostructures usually distinguishing the resulting spin-orbit fields due to broken bulk inversion symmetry, Dresselhaus SOC, and surface inversion asymmetry, Rashba SOC, and focus on their dominant linear dependence in the wave vector, **k** [10, 15]. In this linear regime, with a matching strengths of these SOC it is possible to strongly suppress the spin relaxation [42] and realize a persistent spin helix (PSH) [43, 44] with a controllable spin precession over long distances [45–47].

While typically **k**-cubic SOC contributions (cSOC) in heterostructures are neglected or considered just detrimental perturbations, for example, limiting the stability of PSH [45–47], a more complex picture is emerging. Materials advances suggest that such cSOC, shown in Fig. 1(a), not only has to be included, but may also dominate the normal-state properties [48–57]. However, the role of cSOC in superconducting heterostructures is unexplored. It is unclear if cSOC is detrimental or desirable to key phenomena such as Josephson effect, spin-triplet superconductivity, or Majorana bounds states.

To address this situation and motivate further cSOC studies of superconducting properties, we consider JJs depicted in Fig. 1(b), where s-wave superconductors (S) are separated by a normal region with cSOC which is consistent with the two-dimensional (2D) electron or hole gas, confined along the z-axis [48, 53]. While the commonly-expected current-phase relation (CPR) is $I(\varphi) = I_c \sin(\varphi + \varphi_0)$ [19, 58], where I_c is the JJ critical current and φ_0 the anomalous phase ($\varphi_0 \neq 0, \pi$), we reveal that CPR can be strongly anharmonic and host Majorana bound states. Instead of the p-wave superconducting correlations for linear SOC, their f-wave sym-

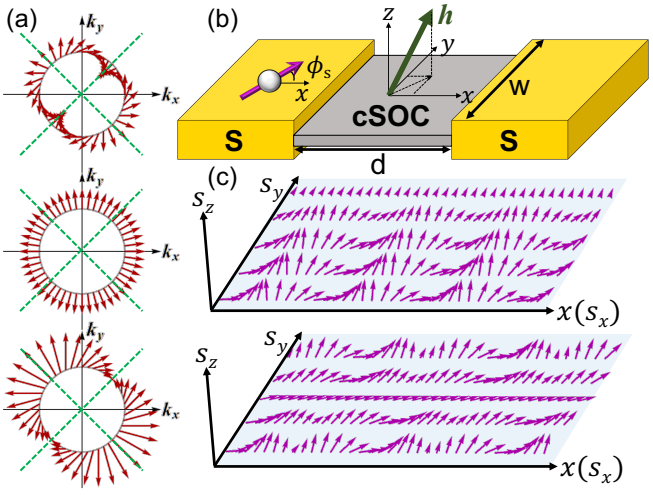

FIG. 1. (a) Spin-orbit fields in k-space for Rashba cubic spin-orbit coupling (cSOC) ($\alpha_c = -1$), Dresselhaus cSOC ($\beta_c = -1$, middle), and both ($\alpha_c = \beta_c = -1$, bottom). (b) Schematic of the Josephson junction. The middle region hosts cSOC and an effective Zeeman field, **h**, between the two s-wave superconductors (S). (c) Spin textures in the cSOC region resulting from the normal-incident electrons with in-plane spin orientations [see Fig. 1(b)] when S is at normal-state, the upper (lower) panel $\alpha_c = 1$, $\beta_c = 0$ ($\alpha_c = \beta_c = 1$). The in-plane spin orientations of the incident electrons ϕ_s are from 0 (bottom row) to $\pi/2$ (top row).

metry is the fingerprint of cSOC.

To study cSOC, we consider an effective Hamiltonian $H = \frac{1}{2}\int d\mathbf{p}\ \hat{\psi}^\dagger(\mathbf{p})H(\mathbf{p})\hat{\psi}(\mathbf{p})$, where $H(\mathbf{p}) = \mathbf{p}^2/2m^* + \boldsymbol{\sigma}\cdot\mathbf{h} + H_{\rm cSOC}(\mathbf{p})$, with momentum, $\mathbf{p} = (p_x, p_y, 0)$ [see Fig. 1(b)], effective mass, m^*, Pauli matrices, $\boldsymbol{\sigma}$, effective Zeeman field, $\mathbf{h}$, realized from an externally applied magnetic field or through magnetic proximity effect [6, 59], and cSOC term [48, 49, 53, 54] $H_{\rm cSOC}(\mathbf{p}) = \frac{i\alpha_c}{2\hbar^3}(p_-^3\sigma_+ - p_+^3\sigma_-) - \frac{\beta_c}{2\hbar^3}(p_-^2 p_+\sigma_+ + p_+^2 p_-\sigma_-)$, expressed using cSOC strengths α_c and β_c, for Rashba and Dresselhaus terms, where $p_\pm = p_x \pm ip_y$, and $\sigma_\pm = \sigma_x \pm i\sigma_y$. The field operator in spin space is given by $\hat{\psi}(\mathbf{p}) = [\psi_\uparrow(\mathbf{p}), \psi_\downarrow(\mathbf{p})]^{\rm T}$, with $\uparrow, \downarrow$ spin projections.

To describe S regions in Fig. 1(b), we use an s-wave BCS model with a two-electron amplitude in spin-Nambu space $\Delta\langle\psi_\uparrow^\dagger\psi_\downarrow^\dagger\rangle$ + H.c., given by the effective Hamiltonian in particle-hole space $\mathcal{H}(\mathbf{p}) = \begin{pmatrix} H(\mathbf{p}) - \mu\hat{1} & \hat{\Delta} \\ \hat{\Delta}^\dagger & -H^\dagger(-\mathbf{p}) + \mu\hat{1} \end{pmatrix}$, where μ is the chemical potential and $\hat{\Delta}$ is a 2×2 gap matrix in spin space. The field operators in the rotated particle-hole and spin basis are $\hat{\psi} = (\psi_\uparrow, \psi_\downarrow, \psi_\downarrow^\dagger, -\psi_\uparrow^\dagger)^{\rm T}$.

To calculate the charge current, we use its quantum definition where no charge sink or source is present. Therefore, the time variation of charge density vanishes, $\partial_t\rho_{\rm c} \equiv 0 = \lim_{\mathbf{r}\to\mathbf{r}'}\sum_{\sigma\tau\sigma'\tau'}[\psi_{\sigma\tau}^\dagger(\mathbf{r}')\mathcal{H}_{\sigma\tau\sigma'\tau'}(\mathbf{r})\psi_{\sigma'\tau'}(\mathbf{r}) - \psi_{\sigma\tau}^\dagger(\mathbf{r}')\mathcal{H}_{\sigma\tau\sigma'\tau'}^\dagger(\mathbf{r}')\psi_{\sigma'\tau'}(\mathbf{r})]$. $\mathcal{H}_{\sigma\tau\sigma'\tau'}$ is the component form of $\mathcal{H}$, with spin (particle-hole) label σ (τ), and and $\mathbf{r} \equiv (x, y, 0)$. From the current conservation, the charge current density is, $\mathbf{J} = \int d\mathbf{r}\{\hat{\psi}^\dagger(\mathbf{r})\overrightarrow{\mathcal{H}}(\mathbf{r})\hat{\psi}(\mathbf{r}) - \hat{\psi}^\dagger(\mathbf{r})\overleftarrow{\mathcal{H}}(\mathbf{r})\hat{\psi}(\mathbf{r})\}$, where $\mathcal{H}(\mathbf{r})$ is obtained by substituting $\mathbf{p} \equiv -i\hbar(\partial_x, \partial_y, 0)$. The arrow directions indicate the specific wavefunctions that the $\mathcal{H}$ operates on. By an exact diagonalization of $\mathcal{H}$, we obtain spinor wavefunctions $\hat{\psi}^{l,r,m}(\mathbf{p})$ within the left ($x < 0$) and right ($x > d$) S region and the middle normal region ($0 < x < d$) in Fig. 1(b). The wavefunctions and generalized velocity operators $v_x^{l,r,m}$ are continuous at the junctions, i.e., $\hat{\psi}^l{=}\hat{\psi}^m|_{x=0}$, $\hat{\psi}^m{=}\hat{\psi}^r|_{x=d}$, $v_x^l\hat{\psi}^l{=}v_x^m\hat{\psi}^r|_{x=0}$, and $v_x^m\hat{\psi}^m{=}v_x^r\hat{\psi}^r|_{x=d}$. The spinor wavefunctions are given in the Supplmental Material [60].

The complexity of $\mathcal{H}$ precludes simple solutions and we evaluate the wavefunctions and supercurrent numerically. To reduce the edge effects, we consider Fig. 1(b) geometry with $W/d \gg 1$ [61]. This approach has been successfully used to study supercurrent in junctions with PSH, Weyl semimetals, phosphorene, and twisted bilayer graphene [62–68]. The calculated supercurrent is normalized by $I_0 = 2|e\Delta|/\hbar$, where e is the electron charge, and Δ the energy gap in S. The energies are normalized by Δ, lengths by $\xi_{\rm S} = \hbar/\sqrt{2m^*\Delta}$, cSOC strengths by $\Delta\xi_{\rm S}^3$. The junction length is set at $d = 0.3\xi_{\rm S}$.

To investigate the role of cSOC on the ground-state Josephson energy, $E_{\rm GS}$, and the CPR obtained from the supercurrent $I(\varphi) \propto \partial E_{\rm GS}/\partial\varphi$, we first consider a simple situation with only Rashba cSOC ($\alpha_c \neq 0$, $\beta_c = 0$) and effective Zeeman field h_x ($h_y = h_z = 0$). The evolution of $E_{\rm GS}$ with $|h_x|$, where its minima are denoted by dots in Fig. 2(a), shows a continuous transition from $\varphi = 0$ to π state (blue to green dot). For $\varphi_0 \neq 0$, $E_{\rm GS}$ minima come in pairs at $\pm\varphi_0$ [69]. The corresponding CPR reveals in Fig. 2(b) a competition between the standard, $\sin\varphi$, and the next harmonic, $\sin 2\varphi$, resulting in $I(-\varphi) = -I(\varphi)$. There is no spontaneous current expected in a Josephson junction with SOC, $I(\varphi = 0) = 0$, but only I_c reversal with h_x. Such a scenario of a continuous and symmetric 0-π transition is well studied without SOC in S/ferromagnet/S JJs due to the changes in the effective magnetization or a thickness of the magnetic region [70–77].

While our previous results suggest no direct cSOC influence on CPR, a simple in-plane rotation of $\mathbf{h}$, $h_x = 0$, $h_y \neq 0$, drastically changes this behavior. This is shown in Figs. 3(b) where, at fixed $|h_y| = 2.4\Delta$, we see a peculiar influence of a finite Rashba cSOC which is responsible for the anomalous Josephson effect with spontaneous current, $I(\varphi = 0) \neq 0$, and strong anharmonic CPR that cannot be described by $I(\varphi) = I_c\sin(\varphi + \varphi_0)$. Unlike in Fig. 3(a), a relative sign between $\alpha_{\rm c}$ and h alters the CPR and Josephson energy, where the ground states φ_0 appear at single points [green, red dots in Fig. 3(a)], consistent with $\varphi_0 \propto \alpha_c h_y$.

If instead of $\mu = \Delta$, we consider a regime $\mu \gg \Delta$, the evolution of Josephson energy from Fig. 2(a) changes. While 0-π transitions with $|h_x|$ remain, there are no longer global minima with $\varphi \neq 0, \pi$ and the CPR reveals a stronger anharmonicity. In contrast, for $\mu \gg \Delta$, the

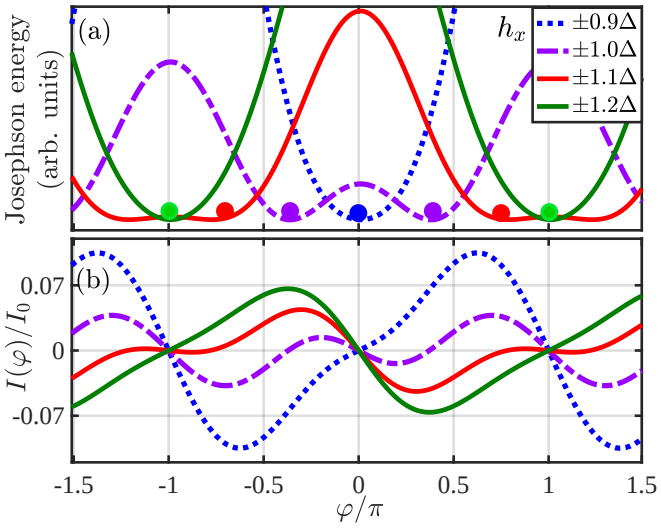

FIG. 2. (a) Josephson energy and (b) associated supercurrent evolution with the superconducting phase difference φ. Zeeman field values, h_x, are chosen near a 0-π transition. The other parameters are $\alpha_{\rm c} = \pm 0.1$ and $\beta_{\rm c} = 0$, $\mu = \Delta$, $h_y = 0$.

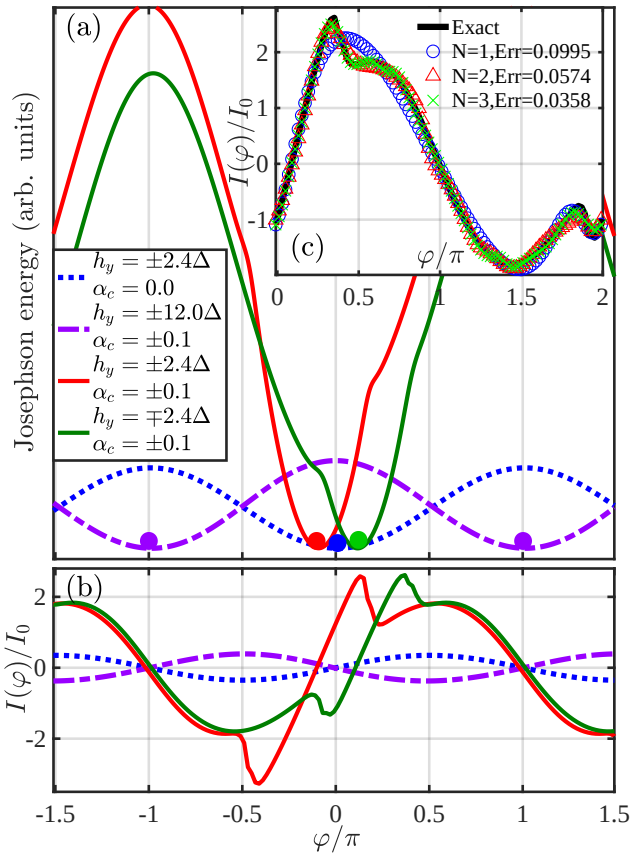

FIG. 3. (a) Josephson energy and (b) related supercurrent evolution with the superconducting phase difference φ Zeeman field, h_y, at a fixed magnitude and varying Rashba cSOC strength α_c are considered. The other parameters are $\beta_c = 0$, $\mu = \Delta$, $h_x = 0$. (c) Three fits to the green curve in (b) using the generalized CPR from Eq. (1) with $N = 1, 2, 3$ harmonics.

anomalous Josephson effect from Fig. 3 remains robust and similar φ_0 states are accessible (see Ref. [60]).

Simple harmonics used to describe anharmonic CPR in high-temperature superconductors [78, 79] here are not very suitable. By generalizing a short-junction limit for CPR [77, 78, 80], we identify a much more compact form where only a small number of terms gives an accurate description. To recognize the importance of SOC and two nondegenerate spin channels, σ, we write

$$I(\varphi) \approx \sum_{n=1}^{N} \sum_{\sigma=\pm} \frac{I_n^\sigma \sin(n\varphi + \varphi_{0n}^\sigma)}{\sqrt{1 - \tau_n^\sigma \sin^2(n\varphi/2 + \varphi_{0n}^\sigma/2)}}, \quad (1)$$

where τ_n^σ is the normal region transparency for spin channel σ. With only few lowest terms in this expansion ($N = 1, 2, 3$), shown in Fig. 3(c) with the corresponding errors, it is possible to very accurately describe strong CPR anharmonicities for anomalous Josephson effect. To achieve the relative error from $N = 3$ expansion in Eq. (1), in a standard $\{\sin, \cos\}$ expansion, with the corresponding phase shifts as extra fitting parameters, requires $N > 20$ [60].

Key insights into the CPR and an explicit functional dependence for the φ_0 state is obtained by a systematic $I(\varphi)$ symmetry analysis with respect to the cSOC (α_c, β_c) and Zeeman field or, equivalently, magnetization ($h_{x,y,z}$) parameters [60]. We find that h_z plays no role in inducing the φ_0 state, it only produces $I(\varphi)$ reversals, explaining our focus on $h_z = 0$ [Figs. 2 and 3].

These properties are expressed as an effective phase shift to a sinusoidal CPR, $\sin(\varphi+\varphi_0)$, extracted from Eq. (1). We again distinguish small- and large-μ regime ($\mu = \Delta$ v.s. $\mu = 10\Delta$). In the first case, for the JJ geometry from Fig. 1, we obtain

$$\varphi_0 \propto \Gamma_y \left(\alpha_c^2 + \Gamma_1 \beta_c^2\right) h_x \beta_c + \Gamma_x \left(\alpha_c^2 - \Gamma_2 \beta_c^2\right) h_y \alpha_c, \quad (2)$$

where the parameters $\Gamma_{1,2,x,y}$ are introduced through their relations, $\Gamma_2 > \Gamma_1$, $\Gamma_1 < 1$, $\Gamma_2 > 1$, $\Gamma_y(h_y = 0) = \Gamma_x(h_x = 0) = 1$, $\Gamma_y(h_y \neq 0) < 1$, $\Gamma_x(h_x \neq 0) < 1$. These relations are modified as μ and $\mathbf{h}$ change. For $\mu \gg \Delta$, the functional dependence for the φ_0 state is simplified

$$\varphi_0 \propto \left(\alpha_c^2 - \Gamma_1 \beta_c^2\right) h_x \beta_c + \left(\alpha_c^2 - \Gamma_2 \beta_c^2\right) h_y \alpha_c, \quad (3)$$

where $\Gamma_2 > \Gamma_1$ and $\Gamma_{1,2} > 1$. Therefore, φ_0 state occurs when $\mathbf{h}$ shifts $\mathbf{p} \perp \boldsymbol{I}(\varphi)$ and thus alters the SOC [60].

Taken together, these results reveal that cSOC in JJ supports a large tunability of the Josephson energy, anharmonic CPR, and the anomalous phase, key to many applications, from post-CMOS logic, superconducting spintronics, quiet qubits, and topological quantum computing. Realizing π states in JJs is desirable for improving rapid single flux quantum (RSFQ) logic, with operation > 100 GHz [81, 82] and enhancing coherence by decoupling superconducting qubits from the environment [83]. However, common approaches for π states using JJs combining s- and d-wave superconductors or JJs with ferromagnetic regions [78, 79] pose various limitations. Instead, extensively studied gate-tunable SOC [10, 38, 45, 53, 54, 84], could allow not only a fast transformation between 0 and π states in JJs with cSOC, but also an arbitrary φ_0 state to tailor desirable CPR.

An insight to the phase evolution and circuit operation of JJs with cSOC is provided by generalizing the classical model of resistively and capacitively shunted junction (RSCJ) [85]. The total current, i, is the sum of the displacement current across the capacitance, C, normal current characterized by the resistance, R, and $I(\varphi)$, $\frac{\phi_0}{2\pi} C \frac{d^2\varphi}{dt^2} + \frac{\phi_0}{2\pi R} \frac{d\varphi}{dt} + I(\varphi) = i$, where ϕ_0 is the magnetic flux quantum and $I(\varphi)$ yields a generally anharmonic CPR, as shown from Eq. (1), which can support 0, π, and tunable φ_0 states. As we have seen from Figs. 2 and 3, this CPR tunability is accompanied by the changes in Josephson energy, which in turn is responsible for the changes in effective values of C, R, and the nonlinear Josephson inductance. This JJ tunability complements using voltage or flux control [86, 87].

In JJs with ferromagnetic regions, I_c is the tunable I_c by changing the underlying magnetic state [32, 88, 89]. In JJs with cSOC, tuning I_c could be realized through gate control by changing the relative strengths of α_c and β_c, even at zero Zeeman field. This is shown in Fig. 4 by calculating Max$[I(\varphi)]$ with $\varphi \in [0, 2\pi]$. In the low-μ regime, the maximum I_c occurs at slightly curved region near the symmetry lines $|\alpha_c| = |\beta_c|$. For the high-μ regime, the region of maximum I_c evolves into inclined symmetry lines, $|\alpha_c| = \mathcal{A}|\beta_c|$, $\mathcal{A} < 1$. Similar to linear SOC, in the diffusive regime for cSOC, one expects that the minimum in I_c occurs near these symmetry lines because of the presence of long-range spin-triplet supercurrent [63, 90].

We expect that a hallmark of JJs with cSOC goes beyond CPR and will also influence the spin structure and symmetry properties of superconducting proximity effects. Linear SOC is responsible for mixed singlet-triplet superconducting pairing [16], while with Zeeman or exchange field it is possible to favor spin-triplet proximity effects which can become long-range [20, 33] or host Majorana bound states [25, 26]. To explore the proximity effects in the cSOC region, we calculate superconducting pair correlations using the Matsubara representation for the anomalous Green function, $F(\tau; \mathbf{r}, \mathbf{r}')$ [92],

$$F_{ss'}(\tau; \mathbf{r}, \mathbf{r}') = +\langle T_\tau \psi_s(\tau, \mathbf{r}) \psi_{s_1}(0, \mathbf{r}') \rangle (-i\sigma^y_{s_1 s'}), \quad (4)$$

where s, s', s_1 are spin indices, the summation is implied over s_1, τ is the imaginary time, ψ_s is the field operator, and T_τ denotes time ordering of operators [60].

For a translationally invariant SOC region, spin-triplet correlations in Fig. 5, obtained from Eq. (4), provide a striking difference between linear and cubic SOC. Unlike the p-wave symmetry for linear Rashba SOC [Figs. 5(a), 5(b)], we see that the f-wave symmetry is the fingerprint for cSOC, retained with only $\alpha_c \neq 0$ [Figs. 5(c), 5(d)] or both $\alpha_c, \beta_c \neq 0$ [Figs. 5(e), 5(f)]. Remarkably, unlike the commonly-sought p-wave symmetry, we confirm that with a suitable orientation of the Zeeman field cSOC also supports Majorana flat bands [60].

While we are not aware of any Josephson effect experiments in 2D systems dominated by cSOC, our studied parameters are within the range of already reported measurements. Choosing m^* of an electron mass, and $\Delta = 0.2\,\text{meV}$, which is similar for both Al and proximity-induced superconductivity [38, 93], the characteristic length becomes $\xi_S \approx 14\,\text{nm}$. The resulting cSOC strength from Fig. 3(b) with $\alpha_c \Delta \xi_S^3 \approx 50\,\text{eVÅ}^3$ is compatible with the values in 2D electron and hole gases [55, 56]. The Zeeman splitting $2.4 \times 0.2\,\text{meV}$ is available by applying magnetic field in large g-factor materials [10], or from magnetic proximity effects, measured in 2D systems to reach up to $\sim 20\,\text{meV}$ [6]. Even though we have mostly focussed on the tunable Rashba SOC, the Dresselhaus SOC can also be gate tunable [45, 94], offering a further control of the anomalous Josephson effect.

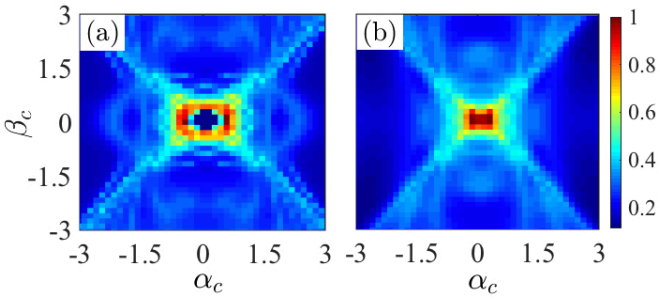

FIG. 4. Normalized critical supercurrent as a function of cSOC strength α_c and β_c for (a) $\mu = \Delta$ and (b) $\mu = 10\Delta$. The Zeeman field is set to zero.

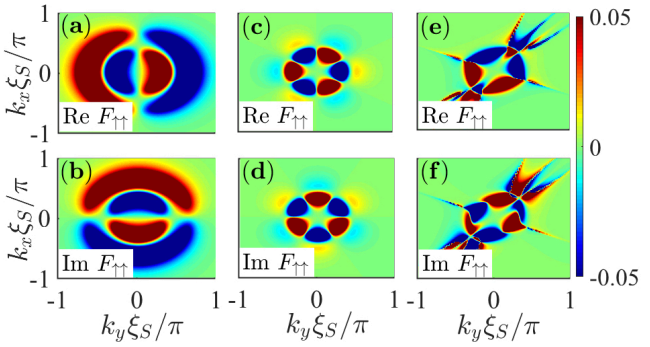

FIG. 5. Real and imaginary parts of equal-spin superconducting correlations in the k-space, $\xi_S = \hbar/\sqrt{2m^*\Delta}$ is the characteristic length. (a), (b) Linear Rashba, $\alpha = 1$. (c), (d) cSOC, $\alpha_c = 1$, $\beta_c = 0$. (e), (f) cSOC, $\alpha_c = \beta_c = 1$. The other parameters are the same for all panels.

Our results reveal that the cSOC in JJs provides versatile opportunities to design superconducting response and test its unexplored manifestations. The anomalous Josephson effect could serve as a sensitive probe to quantify cSOC. While identifying the relevant form of SOC is a challenge even in the normal state [10, 12], in the superconducting state already a modest SOC can give a strong anisotropy in the transport properties [24, 95–97] and enable extracting the resulting SOC. Identifying SOC, either intrinsic, or generated through magnetic textures, remains important for understanding which systems could host Majorana bound states [37, 98–111].

With the advances in gate-tunable structures and novel materials systems [38, 53–56, 93, 112], the functional dependence of the anomalous phase φ_0 and the f-wave superconducting correlations could also enable decoupling of the linear and cubic SOC contributions [60]. For the feasibility of such decoupling, it would be useful to consider methods employed in the studies of the nonlinear Meissner effect [113–120]. Even small corrections to the supercurrent from the magnetic anisotropy of the nonlinear Meissner response offer a sensitive probe to distinguish different paring-state symmetries.

C.S. and I.Ž. were supported by NSF ECCS-1810266,

and I.Ž by DARPA DP18AP900007, and the UB Center for Computational Research.

[1] C. L. Kane and E. J. Mele, Quantum Spin Hall Effect in Graphene, Phys. Rev. Lett. **95**, 226801 (2005).

[2] M. König, S. Wiedmann, C. Brüne, A. Roth, H. Buhmann, L. W. Molenkamp, X.-L. Qi, and S.-C. Zhang, Quantum Spin Hall Insulator State in HgTe Quantum Wells, Science **318**, 766 (2007).

[3] X. Wan, A. M. Turner, A. Vishwanath, and S. Y. Savrasov, Topological semimetal and Fermi-arc surface states in the electronic structure of pyrochlore iridates, Phys. Rev. B **83**, 205101 (2011).

[4] A. A. Burkov and L. Balents, Weyl Semimetal in a Topological Insulator Multilayer, Phys. Rev. Lett. **107**, 127205 (2011).

[5] N. P. Armitage, E. J. Mele, A. Vishwanath, Weyl and Dirac semimetals in three-dimensional solids, Rev. Mod. Phys. **90**, 015011 (2018).

[6] I. Žutić, A. Matos-Abiague, B. Scharf, H. Dery, K. Belashchenko, Proximitized materials, Mater. Today **22**, 85 (2019).

[7] Y. A. Bychkov and E. I. Rashba, Properties of a 2D electron gas with lifted spectral degeneracy, Pis'ma Zh. Eksp. Teor. Fiz. **39**, 66 (1984) [JETP Lett. **39**, 78 (1984)].

[8] R. Winkler, *Spin-Orbit Coupling Effects in Two-Dimensional Electron and Hole Systems* (Springer, New York, 2003).

[9] S. Das Sarma, J. Fabian, X. Hu, I. Žutić, Spin electronics and spin computation, Solid State Commun. **119**, 207 (2001).

[10] I. Žutić, J. Fabian, and S. Das Sarma, Spintronics: Fundamentals and applications, Rev. Mod. Phys. **76**, 323 (2004).

[11] R. Hanson, L. P. Kouwenhoven, J. R. Petta, S. Tarucha, and L. M. K. Vandersypen, Spins in few-electron quantum dots, Rev. Mod. Phys. **79**, 1217 (2007).

[12] J. Fabian, A. Matos-Abiague, C. Ertler, P. Stano, and I. Žutić, Semiconductor Spintronics, Acta Phys. Slov. **57**, 565 (2007).

[13] Di Xiao, M.-C. Chang, and Q. Niu, Berry phase effects on electronic properties, Rev. Mod. Phys. **82**, 1959 (2010).

[14] J. Sinova, S. O. Valenzuela, J. Wunderlich, C. H. Back, and T. Jungwirth, Spin Hall effects, Rev. Mod. Phys. **87**, 1213 (2015).

[15] J. Schliemann, Colloquium: Persistent spin textures in semiconductor nanostructures, Rev. Mod. Phys. **89**, 011001 (2017).

[16] L. P. Gor'kov and E. I. Rashba, Superconducting 2D System with Lifted Spin Degeneracy: Mixed Singlet-Triplet State, Phys. Rev. Lett. **87**, 037004 (2001).

[17] K. V. Samokhin, Paramagnetic Properties of Noncentrosymmetric Superconductors: Application to $CePt_3Si$, Phys. Rev. Lett. **94**, 027004 (2005); P. M. R. Brydon, L. Wang, M. Weinert, and D. F. Agterberg, Pairing of $j = 3 = 2$ Fermions in Half-Heusler Superconductors, Phys. Rev. Lett. **116** 177001 (2016).

[18] A. A. Reynoso, G. Usaj, C. A. Balseiro, D. Feinberg, and M. Avignon, Anomalous Josephson Current in Junctions with Spin Polarizing Quantum Point Contacts, Phys. Rev. Lett. **101**, 107001 (2008).

[19] A. Buzdin, Direct Coupling Between Magnetism and Superconducting Current in the Josephson φ_0 Junction, Phys. Rev. Lett. **101**, 107005 (2008); F. Konschelle and A. Buzdin, Magnetic Moment Manipulation by a Josephson Current, Phys. Rev. Lett. **102**, 017001 (2009).

[20] M. Eschrig, Spin-polarized supercurrents for spintronics: A review of current progress, Rep. Prog. Phys. **78**, 104501 (2015).

[21] M. Smidman, M. B. Salamon, H. Q. Yuan, and D. F. Agterberg, Superconductivity and spin-orbit coupling in non-centrosymmetric materials: A review, Rep. Prog. Phys. **80**, 036501 (2017).

[22] I. Martínez, P. Högl, C. González-Ruano, J. P. Cascales, C. Tiusan, Y. Lu, and M. Hehn, A. Matos-Abiague, J. Fabian, I. Žutić, and F. G. Aliev Interfacial Spin-Orbit Coupling: A Platform for Superconducting Spintronics, Phys. Rev. Applied **13**, 014030 (2020).

[23] K.-R. Jeon, X. Montiel, S. Komori, C. Ciccarelli, J. Haigh, H. Kurebayashi, L. F. Cohen, A. K. Chan, K. D. Stenning, C.-M. Lee, M. G. Blamire, and J. W. A. Robinson, Tunable Pure Spin Supercurrents and the Demonstration of Their Gateability in a Spin-Wave Device, Phys. Rev. X **10**, 031020 (2020).

[24] C. González-Ruano, L. G. Johnsen, D. Caso, C. Tiusan, M. Hehn, N. Banerjee, J. Linder, and F. G. Aliev, Superconductivity-induced change in magnetic anisotropy in epitaxial ferromagnet-superconductor hybrids with spin-orbit interaction, Phys. Rev. B **102**, 020405(R) (2020).

[25] R. M. Lutchyn, J. D. Sau, and S. Das Sarma, Majorana Fermions and a Topological Phase Transition in Semiconductor-Superconductor Heterostructures, Phys. Rev. Lett. **105**, 077001 (2010).

[26] Y. Oreg, G. Refael, and F. von Oppen, Helical Liquids and Majorana Bound States in Quantum Wires, Phys. Rev. Lett. **105**, 177002 (2010).

[27] D. Aasen, M. Hell, R. V. Mishmash, A. Higginbotham, J. Danon, M. Leijnse, T. S. Jespersen, J. A. Folk, C. M. Marcus, K. Flensberg, and J. Alicea, Milestones Toward Majorana-Based Quantum Computing, Phys. Rev. X **6**, 031016 (2016).

[28] R. S. Keizer, S. T. B. Goennenwein, T. M. Klapwijk, G. Miao, G. Xiao, and A. A. Gupta, A spin triplet supercurrent through the half-metallic ferromagnet CrO_2, Nature **439**, 825 (2006).

[29] J. W. A. Robinson, J. D. S. Witt, and M. G. Blamire, Controlled Injection of Spin-Triplet Supercurrents into a Strong Ferromagnet, Science **329**, 59 (2010).

[30] T. S. Khaire, M. A. Khasawneh, W. P. Pratt, Jr., and N. O. Birge, Observation of Spin-Triplet Superconductivity in Co-Based Josephson Junctions, Phys. Rev. Lett. **104**, 137002 (2010).

[31] N. Banerjee, J. W. A. Robinson, and M. G. Blamire, Reversible control of spin-polarized supercurrents in ferromagnetic Josephson junctions, Nat. Commun. **5**, 4771 (2014).

[32] E. C. Gingrich, B. M. Niedzielski, J. A. Glick, Y. Wang, D. L. Miller, R. Loloee, W. P. Pratt, Jr., and N. O. Birge, Controllable $0-\pi$ Josephson junctions containing a ferromagnetic spin valve, Nat. Phys. **12**, 564 (2016).

[33] J. Linder and J. W. A. Robinson, Superconducting spintronics, Nat. Phys. **11**, 307 (2015).

[34] L. P. Rokhinson, X. Liu, and J. K. Furdyna, The fractional a.c. Josephson effect in a semiconductor-superconductor nanowire as a signature of Majorana particles, Nat. Phys. **8**, 795 (2012).

[35] A. Fornieri, A. M. Whiticar, F. Setiawan, E. Portolés, A. C. C. Drachmann, A. Keselman, S. Gronin, C. Thomas, T. Wang, R. Kallaher, G. C. Gardner, E. Berg, M. J. Manfra, A. Stern, C. M. Marcus, and F. Nichele, Evidence of topological superconductivity in planar Josephson junctions, Nature **569**, 89 (2019).

[36] H. Ren, F. Pientka, S. Hart, A. Pierce, M. Kosowsky, L. Lunczer, R. Schlereth, B. Scharf, E. M. Hankiewicz, L. W. Molenkamp, B. I. Halperin, and A. Yacoby, Topological superconductivity in a phase-controlled Josephson junction, Nature **569**, 93 (2019).

[37] M. M. Desjardins, L. C. Contamin, M. R. Delbecq, M. C. Dartiailh, L. E. Bruhat, T. Cubaynes, J. J. Viennot, F. Mallet, S. Rohart, A. Thiaville, A. Cottet, and T. Kontos, Synthetic spin-orbit interaction for Majorana devices, Nat. Mater. **18**, 1060 (2019).

[38] M. C. Dartiailh, W. Mayer, J. Yuan, K. S. Wickramasinghe, A. Matos-Abiague, I. Žutić, and J. Shabani, Phase signature of topological transition in Josephson junctions, arXiv:1906.01179.

[39] A. P. Mackenzie, Y. Maeno, The superconductivity of Sr_2RuO_4 and the physics of spin-triplet pairing, Rev. Mod. Phys. **75**, 657 (2003).

[40] A. Pustogow, Y. Luo, A. Chronister, Y.-S. Su, D. A. Sokolov, F. Jerzembeck, A. P. Mackenzie, C. W. Hicks, N. Kikugawa, S. Raghu, E. D. Bauer and S. E. Brown Pronounced drop of ^{17}O NMR Knight shift in superconducting state of Sr_2RuO_4, Nature **574**, 72 (2019); I. Žutić and I. Mazin, Phase-Sensitive Tests of the Pairing State Symmetry in Sr_2RuO_4, Phys. Rev. Lett. **95**, 217004 (2005).

[41] R. Sharma, S. D. Edkins, Z. Wang, A. Kostin, C. Sow, Y. Maeno, A. P. Mackenzie, J. C. S. Davis, and V. Madhavan Momentum-resolved superconducting energy gaps of Sr_2RuO_4 from quasiparticle interference imaging, Proc. Natl. Acad. Sci. U.S.A. **117**, 5222 (2020).

[42] J. Schliemann, J. C. Egues, and D. Loss, Nonballistic Spin-Field-Effect Transistor, Phys. Rev. Lett. **90**, 146801 (2003).

[43] B. A. Bernevig, J. Orenstein, and S.-C. Zhang, Exact SU(2) Symmetry and Persistent Spin Helix in a Spin-Orbit Coupled System, Phys. Rev. Lett. **97**, 236601 (2006).

[44] J. D. Koralek, C. P. Weber, J. Orenstein, B. A. Bernevig, S.-C. Zhang, S. Mack, and D. D. Awschalom, Emergence of the persistent spin helix in semiconductor quantum wells, Nature **458**, 610 (2009).

[45] F. Dettwiler, J. Fu, S. Mack, P. J. Weigele, J. C. Egues, D. D. Awschalom, and D. M. Zumbuhl, Stretchable Persistent Spin Helices in GaAs Quantum Wells, Phys. Rev. X **7**, 031010 (2017).

[46] M. P. Walser, C. Reichl, W. Wegscheider, and G. Salis, Direct mapping of the formation of a persistent spin helix, Nat. Phys. **8**, 757 (2012).

[47] D. Iizasa, M. Kohda, U. Zülicke, J. Nitta, and M. Kammermeier, Enhanced longevity of the spin helix in low-symmetry quantum wells, Phys. Rev. B **101**, 245417 (2020).

[48] R. Winkler, H. Noh, E. Tutuc, and M. Shayegan, Anomalous Rashba spin splitting in two-dimensional hole systems, Phys. Rev. B **65**, 155303 (2002).

[49] J. J. Krich and B. I. Halperin, Cubic Dresselhaus Spin-Orbit Coupling in 2D Electron Quantum Dots, Phys. Rev. Lett. **98**, 226802 (2007).

[50] P. Altmann, F. G. G. Hernandez, G. J. Ferreira, M. Kohda, C. Reichl, W. Wegscheider, and G. Salis, Current-Controlled Spin Precession of Quasistationary Electrons in a Cubic Spin-Orbit Field, Phys. Rev. Lett. 116, 196802 (2016).

[51] K. Yoshizumi, A. Sasaki, M. Kohda, and J. Nitta, Gate-controlled switching between persistent and inverse persistent spin helix states, Appl. Phys. Lett. **108**, 132402 (2016).

[52] M. Kammermeier, P. Wenk, and J. Schliemann, Control of Spin Helix Symmetry in Semiconductor Quantum Wells by Crystal Orientation, Phys. Rev. Lett. **117**, 236801 (2016).

[53] H. Nakamura, T. Koga, and T. Kimura, Experimental Evidence of Cubic Rashba Effect in an Inversion-Symmetric Oxide, Phys. Rev. Lett. **108**, 206601 (2012).

[54] R. Moriya, K. Sawano, Y. Hoshi, S. Masubuchi, Y. Shiraki, A. Wild, C. Neumann, G. Abstreiter, D. Bougeard, T. Koga, and T. Machida, Cubic Rashba Spin-Orbit Interaction of a Two-Dimensional Hole Gas in a Strained-Ge/SiGe Quantum Well, Phys. Rev. Lett. **113**, 0866601 (2014).

[55] R. J. Cottier, B. D. Koehne, J. T. Miracle, D. A. Currie, N. Theodoropoulou, L. Pantelidis, A. Hernandez-Robles, and A. Ponce, Strong spin-orbit interactions in a correlated two-dimensional electron system formed in $SrTiO_3$(001) films grown epitaxially on p-Si(001), Phys. Rev. B **102**, 125423 (2020).

[56] H. Liu, E. Marcellina, A. R. Hamilton, and D. Culcer, Strong Spin-Orbit Contribution to the Hall Coefficient of Two-Dimensional Hole Systems, Phys. Rev. Lett. **121**, 087701 (2018).

[57] V. Brosco, L. Benfatto, E. Cappelluti, C. Grimaldi, Unconventional dc Transport in Rashba Electron Gases, Phys. Rev. Lett. **116**, 166602 (2016).

[58] E. Strambini, A. Iorio, O. Durante, R. Citro, C. Sanz-Fernández, C. Guarcello, I. V. Tokatly, A. Braggio, M. Rocci, N. Ligato, V. Zannier, L. Sorba, F. S. Bergeret, and F. Giazotto, A Josephson phase battery, Nat. Nanotechnol. **15**, 656 (2020).

[59] K. Takiguchi, Le Duc Anh, T. Chiba, T. Koyama, D. Chiba, and M. Tanaka, Giant gate-controlled proximity magnetoresistance in semiconductor-based ferromagnetic/non-magnetic bilayers, Nat. Phys. **15**, 1134 (2019).

[60] See Supplemental Material [link will be provided by publisher] for more details of calculations and analyses, which includes Refs. [10, 63, 65, 66, 92, 114, 119, 121, 122].

[61] M. Alidoust, and K. Halterman, Proximity Induced vortices and long-range triplet supercurrents in ferromagnetic Josephson junctions and spin valves, J. Appl. Phys. **117**, 123906 (2015).

[62] M. Alidoust, and K. Halterman, Supergap and subgap enhanced currents in asymmetric S_1FS_2 Josephson junctions, Phys. Rev. B **102**, 224504 (2020).

[63] M. Alidoust, Critical supercurrent and φ_0 state for probing a persistent spin helix, Phys. Rev. B **101**,

155123 (2020).
[64] M. Alidoust, Self-biased current, magnetic interference response, and superconducting vortices in tilted Weyl semimetals with disorder, Phys. Rev. B **98**, 245418 (2018).
[65] M. Alidoust and K. Halterman, Evolution of pair correlation symmetries and supercurrent reversal in tilted Weyl semimetals, Phys. Rev. B **101**, 035120 (2020).
[66] M. Alidoust, M. Willatzen, and A.-P. Jauho, Strain-engineered Majorana zero energy modes and φ_0 Josephson state in black phosphorus, Phys. Rev. B **98**, 085414 (2018).
[67] M. Alidoust, M. Willatzen, and A.-P. Jauho, Fraunhofer response and supercurrent spin switching in black phosphorus with strain and disorder, Phys. Rev. B **98**, 184505 (2018).
[68] M. Alidoust, A.-P. Jauho, and J. Akola, Josephson effect in graphene bilayers with adjustable relative displacement, Phys. Rev. Res. **2**, 032074(R) (2020).
[69] H. Sickinger, A. Lipman, M. Weides, R. G. Mints, H. Kohlstedt, D. Koelle, R. Kleiner, and E. Goldobin, Experimental Evidence of a φ Josephson Junction, Phys. Rev. Lett. **109**,107002 (2012)
[70] T. Kontos, M. Aprili, J. Lesueur, F. Genêt, B. Stephanidis, and R. Boursier, Josephson Junction through a Thin Ferromagnetic Layer: Negative Coupling, Phys. Rev. Lett. **89**, 137007 (2002).
[71] V. V. Ryazanov, V. A. Oboznov, A. Yu. Rusanov, A. V. Veretennikov, A. A. Golubov, and J. Aarts, Coupling of Two Superconductors Through a Ferromagnet: Evidence for a π Junction, Phys. Rev. Lett. **86**, 2427 (2001).
[72] F. S. Bergeret, A. F. Volkov, and K. B. Efetov, Odd triplet superconductivity and related phenomena in superconductor-ferromagnet structures, Rev. Mod. Phys. **77**, 1321 (2005).
[73] M. Eschrig, J. Kopu, J. C. Cuevas, and G. Schön, Theory of Half-Metal/Superconductor Heterostructures, Phys. Rev. Lett. **90**, 137003 (2003).
[74] K. Halterman, O. T. Valls, and C.-T. Wu, Charge and spin currents in ferromagnetic Josephson junctions Phys. Rev. B **92**, 174516 (2015).
[75] C.-T. Wu and K. Halterman, Spin transport in half-metallic ferromagnet-superconductor junctions, Phys. Rev. B **98**, 054518 (2018).
[76] E. Moen and O. T. Valls Quasiparticle conductance in spin valve Josephson structures, Phys. Rev. **101**, 184522 (2020).
[77] T. Yokoyama, M. Eto, Y. V. Nazarov, Anomalous Josephson effect induced by spin-orbit interaction and Zeeman effect in semiconductor nanowires, Phys. Rev. B **89**, 195407 (2014).
[78] A. A. Golubov, M. Yu. Kupriyanov, and E. Il'ichev, The current-phase relation in Josephson junctions, Rev. Mod. Phys. **76**, 411 (2004).
[79] S. Kashiwaya and Y. Tanaka, Tunnelling effects on surface bound states in unconventional superconductors, Rep. Prog. Phys. **63**, 1641 (2000).
[80] S. Hart, Z. Cui, G. Ménard, M. Deng, A. E. Antipov, R. M. Lutchyn, P. Krogstrup, C. M. Marcus, and K. A. Moler, Current-phase relations of InAs nanowire Josephson junctions: From interacting to multimode regimes, Phys. Rev. B **100**, 064523 (2019).
[81] K. K. Likharev and V. K. Semenov, RSFQ Logic/Memory Family: A New Josephson-Junction Technology for Sub-Terahertz-Clock-Frequency Digital Systems, IEEE Trans. Appl. Supercond. **1**, 3 (1991).
[82] E. Terzioglu and M. R. Beasley, Complementary Josephson Junction Devices and Circuits: A Possible New Approach to Superconducting Electronics, IEEE Trans. Appl. Supercond. **8**, 48 (1998).
[83] T. Yamashita, K. Tanikawa, S. Takahashi, and S. Maekawa, Superconducting Qubit with a Ferromagnetic Josephson Junction, Phys. Rev. Lett. **95**, 097001 (2005).
[84] J. Nitta, T. Akazaki, H. Takayanagi, and T. Enoki, Gate Control of Spin-Orbit Interaction in an Inverted $In_{0.53}Ga_{0.47}As/In_{0.52}Al_{0.48}As$ Heterostructure, Phys. Rev. Lett. **78**, 1335 (1997).
[85] W. C. Stewart, Current-voltage characteristics of Josephson junctions, Appl. Phys. Lett. **12**, 277 (1968).
[86] L. Casparis, M. R. Connolly, M. Kjaergaard, N. J. Pearson, A. Kringhøj, T. W. Larsen, F. Kuemmeth, T. Wang, C. Thomas, S. Gronin, G. C. Gardner, M. J. Manfra, C. M. Marcus, and K. D. Petersson, Nat. Nanotechnol. **13**, 915 (2018).
[87] P. Krantz, M. Kjaergaard, F. Yan, T. P. Orlando, S. Gustavsson, and W. D. Oliver, A Quantum Engineer's Guide to Superconducting Qubits, Appl. Phys. Rev. **6**, 021318 (2019)].
[88] B. Baek, W. H. Rippard, S. P. Benz, S. E. Russek, and P. D. Dresselhaus, Hybrid superconducting-magnetic memory device using competing order parameters, Nat. Commun. **5**, 3888 (2014).
[89] A. Costa, P. Högl, and J. Fabian Magnetoanisotropic Josephson effect due to interfacial spin-orbit fields in superconductor/ferromagnet/superconductor junctions, Phys. Rev. B **95**, 024514 (2017).
[90] M. Alidoust and K. Halterman, Spontaneous edge accumulation of spin currents in finite-size two-dimensional diffusive spin-orbit coupled SFS heterostructures, New J. Phys. **17**, 033001 (2015).
[91] M. Alidoust and K. Halterman, Long-range spin-triplet correlations and edge spin currents in diffusive spin-orbit coupled SNS hybrids with a single spin-active interface, J. Phys: Cond. Matt. **27**, 235301 (2015).
[92] A. Zagoskin, *Quantum Theory of Many-Body Systems*, 2nd Ed. (Springer, New York, 2014).
[93] W. Mayer, M. C. Dartiailh, J. Yuan, K. S. Wickramasinghe, E. Rossi, and J. Shabani, Gate controlled anomalous phase shift in Al/InAs Josephson junctions, Nat. Commun. **11**, 21 (2020).
[94] S. V. Iordanskii, Y. B. Lyanda-Geller, and G. E. Pikus, Weak Localization in Quantum Wells with Spin-Orbit Interaction, JETP Lett. **60**, 206 (1994).
[95] I. Högl, A. Matos-Abiague, I. Žutić, and J. Fabian, Magnetoanisotropic Andreev Reflection in Ferromagnet/Superconductor, Phys. Rev. Lett. **115**, 116601 (2015).
[96] I. Martnez, P. Högl, C. González-Ruano, J. Pedro Cascales, C. Tiusan, Y. Lu, M. Hehn, A. Matos-Abiague, J. Fabian, I. Žutić and F. G. Aliev, Interfacial Spin-Orbit Coupling: A Platform for Superconducting Spintronics, Phys. Rev. Applied **13**, 014030 (2020).
[97] T. Vezin, C. Shen, J. E. Han, and I. Žutić, Enhanced spin-triplet pairing in magnetic junctions with s-wave superconductors, Phys. Rev. B **101**, 014515 (2020).
[98] B. Scharf, F. Pientka, H. Ren, A. Yacoby, and E. M. Hankiewicz, Tuning topological superconductivity

in phase-controlled Josephson junctions with Rashba and Dresselhaus spin-orbit coupling, Phys. Rev. B **99**, 214503 (2019).

[99] J. D. Pakizer, B. Scharf, and A. Matos-Abiague, Crystalline Anisotropic Topological Superconductivity in Planar Josephson Junctions, arXiv:2007.03498.

[100] G. L. Fatin, A. Matos-Abiague, B. Scharf, and I. Žutić, Wireless Majorana Bound States: From Magnetic Tunability to Braiding, Phys. Rev. Lett. **117**, 077002 (2016).

[101] A. Matos-Abiague, J. Shabani, A. D. Kent, G. L. Fatin, B. Scharf, and I. Žutić, Tunable magnetic Textures: From Majorana bound states to braiding, Solid State Commun. **262**, 1 (2017).

[102] F. Ronetti, K. Plekhanov, D. Loss, and J. Klinovaja, Magnetically confined bound states in Rashba systems, Phys. Rev. Research **2**, 022052(R) (2020).

[103] J. Klinovaja, P. Stano, and D. Loss, Transition from Fractional to Majorana Fermions in Rashba Nanowires, Phys. Rev. Lett. **109**, 236801 (2012).

[104] T. Zhou, N. Mohanta, J. E. Han, A. Matos-Abiague, and I. Žutić, Tunable magnetic textures in spin valves: From spintronics to Majorana bound states, Phys. Rev. B **99**, 134505 (2019).

[105] N. Mohanta, T. Zhou, J.-W. Xu, J. E. Han, A. D. Kent, J. Shabani, I. Žutić, and A. Matos-Abiague, Electrical Control of Majorana Bound States Using Magnetic Stripes, Phys. Rev. Applied **12**, 034048 (2019).

[106] S. Turcotte, S. Boutin, J. Camirand Lemyre, I. Garate, and M. Pioro-Ladriére, Optimized micromagnet geometries for Majorana zero modes in low g-factor materials, Phys. Rev. B **102**, 125425 (2020).

[107] Y. Jiang, E. J. de Jong, V. van de Sande, S. Gazibegovic, G. Badawy, E. P. A. M. Bakkers, and S. M. Frolov, Hysteretic magnetoresistance in nanowire devices due to stray fields induced by micromagnets, Nanotechnology **32**, 095001 (2021).

[108] S. Rex, I. V. Gornyi, and A. D. Mirlin, Majorana modes in emergent-wire phases of helical and cycloidal magnet-superconductor hybrids, Phys. Rev. B **102**, 224501 (2020).

[109] V. Kornich, M. G. Vavilov, M. Friesen, M. A. Eriksson, and S. N. Coppersmith, Majorana bound states in nanowire-superconductor hybrid systems in periodic magnetic fields, Phys. Rev. B **101**, 125414 (2020).

[110] N. Mohanta, S. Okamoto, and E. Dagotto, Skyrmion Control of Majorana States in Planar Josephson Junctions, arXiv:2012.13502.

[111] N. Mohanta, A. P. Kampf, and T. Kopp, Supercurrent as a probe for topological superconductivity in magnetic adatom chains, Phys. Rev. B **97**, 214507 (2018).

[112] A. Assouline, C. Feuillet-Palma, N. Bergeal, T. Zhang, A. Mottaghizadeh, A. Zimmers, E. Lhuillier, M. Marangolo, M. Eddrief, P. Atkinson, M. Aprili, H. Aubin, Spin-Orbit induced phase-shift in Bi_2Se_3 Josephson junctions, Nat. Comm. **10**, 126 (2019).

[113] D. Xu, S. K. Yip, and J. A. Sauls, The Nonlinear Meissner Effect in Unconventional Superconductors, Phys. Rev. B **51**, 16233 (1995).

[114] S. Bae, Y. Tan, A. P. Zhuravel, L. Zhang, S. Zeng, Y. Liu, T. A. Lograsso, Ariando, T. Venkatesan, and S. M. Anlage, Dielectric resonator method for determining gap symmetry of superconductors through anisotropic nonlinear Meissner effect, Rev. Sci. Instrum. **90**, 043901 (2019).

[115] A. P. Zhuravel, B. G. Ghamsari, C. Kurter, P. Jung, S. Remillard, J. Abrahams, A. V. Lukashenko, A. V. Ustinov, and S. M. Anlage, Imaging the Anisotropic Nonlinear Meissner Effect in Nodal $YBa_2Cu_3O7 - \delta$ Thin-Film Superconductors, Phys. Rev. Lett. **110**, 087002 (2013).

[116] R. Prozorov and R. W Giannetta, Magnetic penetration depth in unconventional superconductors, Supercond. Sci. Technol. **19**, R41 (2006).

[117] K. Halterman, O. T. Valls, and I. Žutić Angular dependence of the penetration depth in unconventional superconductors, Phys. Rev. B **63**, 014501 (2000).

[118] A. Bhattacharya, I. Žutić, A. M.Goldman, O. T. Valls, U. Welp, and B. Veal, Angular Dependence of the Nonlinear Magnetic Moment of $YBa_2Cu_3O6.95$in the Meissner State, Phys. Rev. Lett. **82**, 3132 (1999).

[119] I. Žutić and O. T. Valls, Superconducting-gap-node spectroscopy using nonlinear electrodynamics, Phys. Rev. B **56**, 11279 (1997).

[120] I. Žutić and O. T. Valls, Low-frequency nonlinear magnetic response of an unconventional superconductor, Phys. Rev. B **58**, 8738 (1998).

[121] M. Alidoust, M. Willatzen, A.-P. Jauho, Control of superconducting pairing symmetries in monolayer black phosphorus, Phys. Rev. B **99**, 125417 (2019).

[122] K. Halterman, O. T. Valls, and I. Žutić, Reanalysis of the magnetic field dependence of the penetration depth: Observation of the nonlinear Meissner effect, Phys. Rev. B **63**, 180405(R) (2001).